ON THE MULTI-MODAL GROWTH OF DISTURBANCES IN A LAMINAR SEPARATION BUBBLE SUBJECTED TO FREESTREAM TURBULENCE

Tomek Jaroslawski*, Olivier Vermeersch and Maxime Forte
Dept. of Multi-Physics for Energetics
ONERA
Toulouse, France
thomas.jaroslawski@onera.fr*, olivier.vermeersch@onera.fr, maxime.forte@onera.fr

Erwin Gowree and Jean-Marc Moschetta
Dept. of Aerodynamics and Propulsion
ISAE-SUPAERO
Toulouse, France
erwin-ricky.gowree@isaesupaero.fr, jean-marc.moschetta@isaesupaero.fr

ABSTRACT

Experiments were conducted to study the transition and flow development in a laminar separation bubble (LSB) formed on an aerofoil. The effects of a wide range of freestream turbulence intensity ($0.15\% < Tu < 6.26\%$) and streamwise integral length scale ($4.6mm < \Lambda_u < 17.2mm$) are considered. The coexistence of a modal instability due to the LSB and a non-modal instability caused by streaks generated by freestream turbulence is observed. The presence of streaks in the boundary layer modifies the mean flow topology of the bubble. These changes in the mean flow field result in the modification of the convective disturbance growth, where an increase in turbulence intensity is found to dampen the growth of the modal instability. For a relatively fixed level of Tu, the variation of Λ_u has modest effects, however a slight advancement of the non-linear growth of disturbances and eventual breakdown with the decrease in Λ_u is observed. The data shows that the streamwise growth of the disturbance energy is exponential for the lowest levels of freestream turbulence and gradually becomes algebraic as the level of freestream turbulence increases. Once a critical turbulence intensity is reached, there is enough energy in the boundary layer to suppress the LSB, which in turn, results in the non-modal instability to take over the transition process. Linear stability analysis is conducted in the fore position of the LSB, and accurately models unstable frequencies and eigenfunctions for configurations subjected to levels of turbulence intensity levels up to 3%. Increasing the Tu resulted in the Reynolds number dependence to increase, suggesting that a viscous, rather than an invicid formulation of the stability equations is appropriate for modeling modal instabilities in the fore portion of the studied LSB.

INTRODUCTION

At low Reynolds numbers ($Re < 5 \times 10^5$) viscous effects are significant, such that the presence of a strong enough adverse pressure gradient can cause a laminar boundary layer to separate from the wall. These types of flows are common in engineering applications such as low-pressure turbines (Volino, 1997) and micro-aerial vehicles (Jaroslawski *et al.*, 2022). The effects of freestream turbulence intensity (Tu) and integral length scale (Λ_u) on boundary layer transition in LSBs have not been addressed to the same extent as for attached boundary layers. Häggmark *et al.* (2000) provided some of the first experimental results on the effects of grid generated freestream turbulence (FST) on an LSB generated over a flat plate subjected to an adverse pressure gradient. They found low frequency streaky structures in the boundary layer upstream of the separation and in the separated shear layer from smoke visualisation and spectral analysis. More recently, Istvan & Yarusevych (2018) experimentally investigated the effects of FST on an LSB formed over a NACA0018 aerofoil for a chord based Reynolds numbers of 80000 and 150000 using Particle Image Velocimetry (PIV). They found that increasing the level of FST leads to a decrease in the chordwise length of the LSB due to a downstream shift of the separation point and an upstream shift of the reattachment point. Hosseinverdi & Fasel (2019) used direct numerical simulations (DNS) to investigate the role of isotropic FST on the hydrodynamic instability mechanisms and laminar to turbulent transition in an LSB. They reported that the FST induced Klebanoff modes (streaks) upstream of the separation location, proposing that the boundary layer transition process was made up of two mechanisms. The first consisted of low frequency Klebanoff modes (streaks) induced by the FST and the second being a Kevin-Helmholtz instability enhanced by the FST. Depending on the level of FST either one or both of these mechanisms would dominate the transition process.

Hence the common notion of the modal instability being "bypassed" appears to be under question as evidence from the above authors suggests the coexistence of two competing transition mechanisms in an LSB. However, there is a lack of knowledge on how freestream turbulence and the integral length scale of turbulence affect the stability of an LSB subjected to FST. The present work investigates the effects of forcing an LSB with a large range of Tu and Λ_u on the flow development, stability and transition of the bubble. The aim of this study is to experimentally investigate the laminar separation bubble, focusing our attention on the coexistence of modal and non-modal instabilities, their interaction and effects on the transition process.

EXPERIMENTAL SETUP

The experiments were conducted at atmospheric conditions in the ONERA Toulouse TRIN 2 subsonic wind tunnel. The maximum freestream turbulence level (measured near the leading edge of the aerofoil, cf. Fig. 1a) in the test section with the aerofoil mounted was found to be below 0.15 %. The freestream velocity was fixed at $U_\infty \cong 6m/s$ for all test configurations, corresponding to a chord based Reynolds number, $Re_c = U_\infty c/\nu$ of 125000. The angle of attack, AoA, was fixed to a value of 2.3° throughout all the experiments. Velocity measurements are acquired using a Dantec Dynamics Streamline Pro system with a 90C10 module and a 55P15 boundary layer probe mounted on a two-dimensional traverse, at a sampling frequency of 25 kHz. Freestream turbulence measurements were conducted using a 5 μm Dantec 55P51 X-Wire probe. Freestream turbulence is generated in a controlled manner using a variety of regular and fractal grids (refer to Fig. 1 b,c) set up in a way such that turbulence interacting with the bubble would be approximately isotropic and homogeneous. The evolution of the grid generated turbulence was characterised before the leading edge and above the aerofoil. The tested configurations are presented in table 1. Infrared Thermography measurements were also conducted to validate the spanwise flow homogeneity of the bubble (which are not presented in the present paper). The experimental setup is presented in Fig. 1a.

Config.	v_{rms}/u_{rms}	$Tu(\%)$	$\Lambda_u(mm)$	$\Lambda_v(mm)$
NG●	0.92	0.15	210	181
C0 ●	0.82	0.64	4.6	3.1
C1 ●	0.91	1.21	8.7	5.5
C2 ●	0.81	1.23	10.3	6.7
C3 ○	0.92	1.31	8.3	5.6
C4 ●	1.07	1.63	12.3	8.3
C5 ●	1.07	2.97	15.4	10.6
C6 ●	1.02	4.16	16.8	11.4
C7 ●	1.10	6.26	17.2	13.3

Table 1. Freestream turbulence test matrix. Turbulence isotropy, turbulence intensity (Tu), streamwise and vertical integral length scale (Λ_u and Λ_v, respectively) at the leading edge of the aerofoil ($x/c = 0$).

LOCAL LINEAR STABILITY ANALYSIS

Linear Stability Theory (LST) has been employed to study the convective streamwise amplification of disturbances in the LSB. The Orr-Sommmerfeld given by Eq. 1, can reliably predict the primary amplification of instability waves for parallel flows and in the fore position of a LSB (Yarusevych & Kotsonis, 2017).

$$\begin{aligned}&\left(U-\frac{\Omega}{\alpha}\right)\left(\frac{d^2\tilde{v}}{dy^2}-\alpha^2\tilde{v}\right)-\frac{d^2U}{dy^2}\tilde{v}\\ &=-\frac{iU_e\delta_1}{\alpha Re_{\delta_1}}\left(\frac{d^4\tilde{v}}{dy^4}-2\alpha^2\frac{d^2\tilde{v}}{dy^2}+\alpha^4\tilde{v}\right)\end{aligned} \tag{1}$$

where Re_{δ_1} is the Reynolds number based on displacement thickness, $\tilde{v}$ is the wall-normal perturbation, Ω is the angular frequency and the complex wave number is defined as $\alpha = \alpha_r + i\alpha_i$, where i is the imaginary unit. When $\alpha_i > 0$ the disturbance is attenuated and amplified when $\alpha_i < 0$.

Calculations were conducted using ONERA's in house stability code, where a spatial formulation of the problem is employed, such that Ω is defined and the eigenvalue problem is solved for α, therefore modelling the convective amplification of single frequency disturbances. Equation 1 is solved numerically using Chebyshev polynomial base functions and the companion matrix technique to treat eigenvalue non-linearity.

The mean streamwise velocity profiles at discrete streamwise locations are used as input for the LST calculations. In the stability analysis the higher order spatial gradients are highly sensitive to noise, therefore hyperbolic tangent fits are used for the calculations. This method has been shown to provide accurate linear stability predictions on HWA velocity profiles of separated shear layers (Boutilier & Yarusevych, 2012).

RESULTS

The mean streamwise velocity and u_{rms} contours (which are composed of 21 streamwise velocity profiles separated by $0.025c$ in the chordwise direction) are presented in Fig. 2a and show the presence of an LSB that extends from $x_S/c = 0.375 \pm 0.05$ to $x_S/c = 0.700 \pm 0.025$ for the natural case. In the presence of freestream turbulence forcing the mean flow toplogy of the LSB changes, in particular a slight delay of boundary layer separation is observed, the height decreases significantly and the mean transition position advances upstream as can be observed in Fig. 2b. At the highest level of Tu (Fig. 2c), no LSB is observed as there is enough energy injected from the freestream turbulence into the boundary layer to suppress the laminar separation. The measurements, in accordance with previous studies (Istvan & Yarusevych, 2018; Simoni *et al.*, 2017; Hosseinverdi & Fasel, 2019), show that with the increase of Tu, the streamwise extent of the separation bubble is reduced. This is a result of an earlier onset of pressure recovery, caused by the shear layer transitioning in the aft position of the LSB.

The power spectral density (PSD) of the streamwise velocity fluctuations was calculated for each configuration, with the chordwise evolution presented in Fig. 4. In the cases where an LSB was present, the PSD exhibits a characteristic frequency band which is amplified downstream (cf. Fig. 4a-c). When the LSB was subjected to FST the chordwise development and distribution of the spectra is significantly modified. First the unstable frequency band is broadened, which is a consequence of significant energy content within a broader range of frequencies in the FST, resulting in measurable velocity fluctuations over a broader frequency range earlier upstream. Second, increasing the freestream turbulence level, results in the unstable frequency band to be slightly shifted to a higher frequency range compared to the natural case. The frequency shift of the wave packet is attributed to the decreased streamwise length and height of the LSB, and has been observed in Hosseinverdi & Fasel (2019).

The effect of increasing the level of Tu on the chordwise evolution of the disturbance energy growth ($E = u_{rms}^2/U_e^2$) is presented in Fig. 3a, where the trend of disturbance growth gradually changes from exponential, at lower levels of Tu, to algebraic for the more extreme Tu levels, where energy saturation is observed earlier. Algebraic or transient growth is associated with a non-modal instability, commonly due to streaks in boundary layer flows subjected to elevated levels of freestream turbulence ($Tu > 1\%$) and has been well documented for zero-pressure gradient attached boundary layers (Matsubara & Alfredsson, 2001; Fransson *et al.*, 2005). These different energy growth behaviours suggest that different instability mechanisms are present in the flow, and their con-

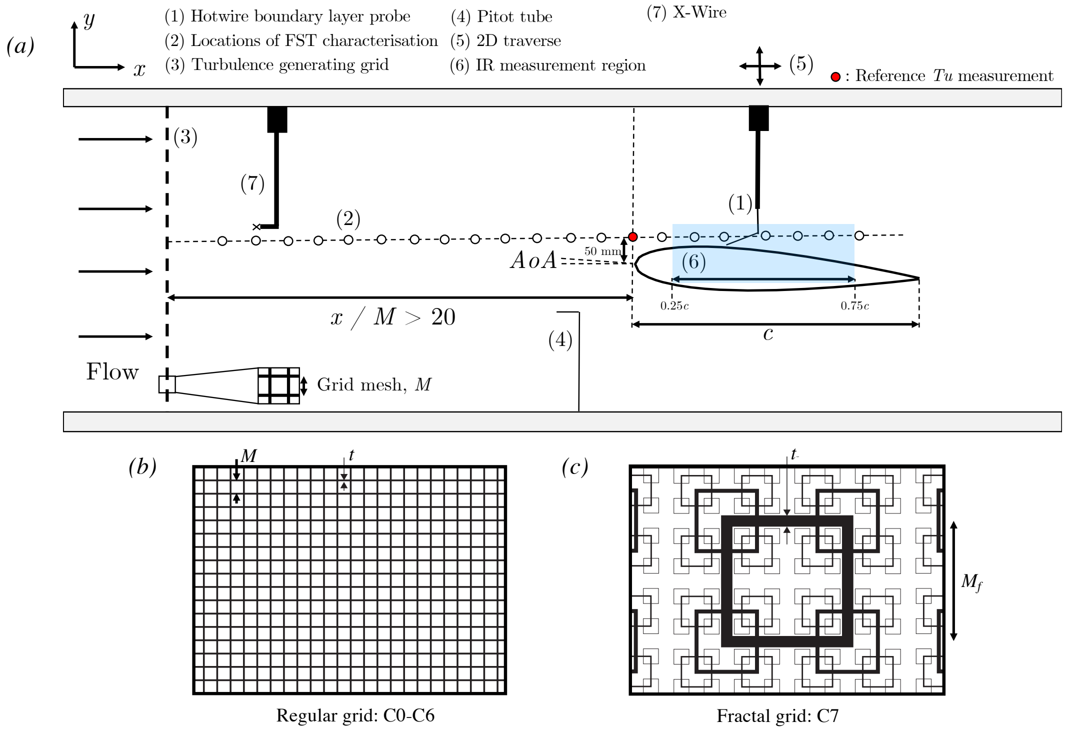

Figure 1. a)Experimental Setup. (b) Schematic of regular grid (configs. C0-C6) and (b) fractal grid (config. C7)

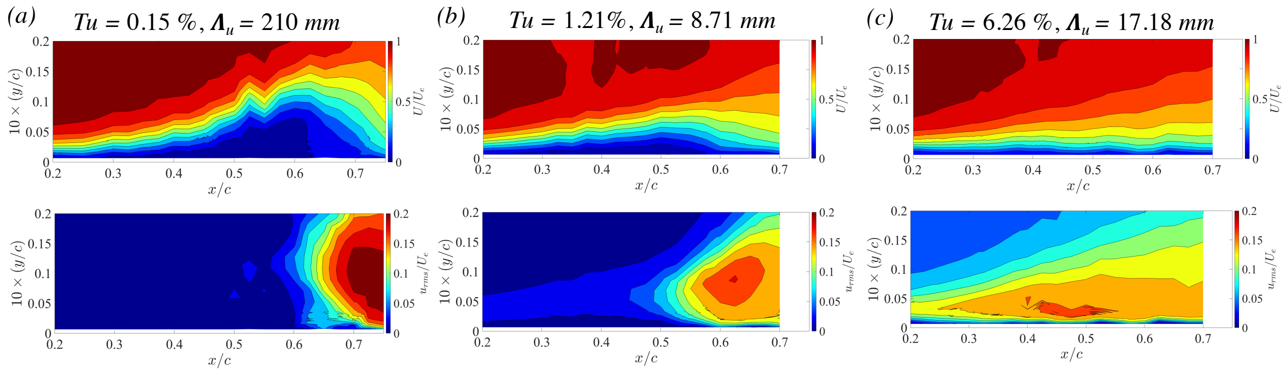

Figure 2. Contours of the mean streamwise velocity (U) and the r.m.s of the fluctuating streamwise velocity (u_{rms}) (a) 0.15% (b) 1.21% and (c) 6.28%.

tribution to the transition process depends on the level of the freestream forcing.

Referring to Fig. 3b, the gradual reduction in the slope of the filtered (bandpass filtered for the most amplified frequencies obtained from the PSD) chordwise energy growth with increasing Tu would suggest that the non-modal instabilities become more dominant, which can be thought of as being in competition with the modal instabilities which grow exponentially. Once the turbulence forcing reaches a critical level, the excited streaks in the boundary layer are too energetic to allow the flow to separate, resulting in the elimination of the modal via the non-modal instability. Damping of the modal disturbance growth is attributed to the mean flow deformation due to the influence of freestream turbulence. In other words, external freestream turbulence forcing reduces the size of the separation bubble, such that the region of instability growth is brought closer to the wall, resulting in damping effects of the disturbances in the shear layer. Previous experiments on forced bubbles, found a damping effect on the disturbance growth. For example, Kurelek *et al.* (2018) found that both tonal and broadband acoustic forcing resulted in the damping of modal disturbances along with Yarusevych & Kotsonis (2017) and Marxen & Henningson (2011) who used a variety of forcing techniques to find similar results.

The impact of the integral length scale for a relatively constant Tu level on the disturbance growth is presented in Fig. 3c, suggesting that the effect of the integral length scale on the growth of disturbances in the LSB is very modest. Achieving constant levels of Tu with a varying Λ_u is an experimental challenge, as shown by by Fransson & Shahinfar (2020). In the present work, three cases which have a very small variation in Tu and a larger variation in Λ_u are investigated. It is observed that an increase in Λ_u at the leading edge of the aerofoil for an almost constant Tu appears to delay the growth and eventual saturation and breakdown of the disturbances. This is in agreement Breuer (2018), who suggested that the smaller scales were closer to that of the shear layer, resulting in the receptivity of the boundary layer to increase. Hosseinverdi & Fasel (2019) briefly suggested that the integral length scales ranging from $0.9\delta_1$ to $3\delta_1$ had little effect on the energy growth relative to the Tu, which is observed in the experimental results here. Furthermore, a smaller integral length scale resulted in a

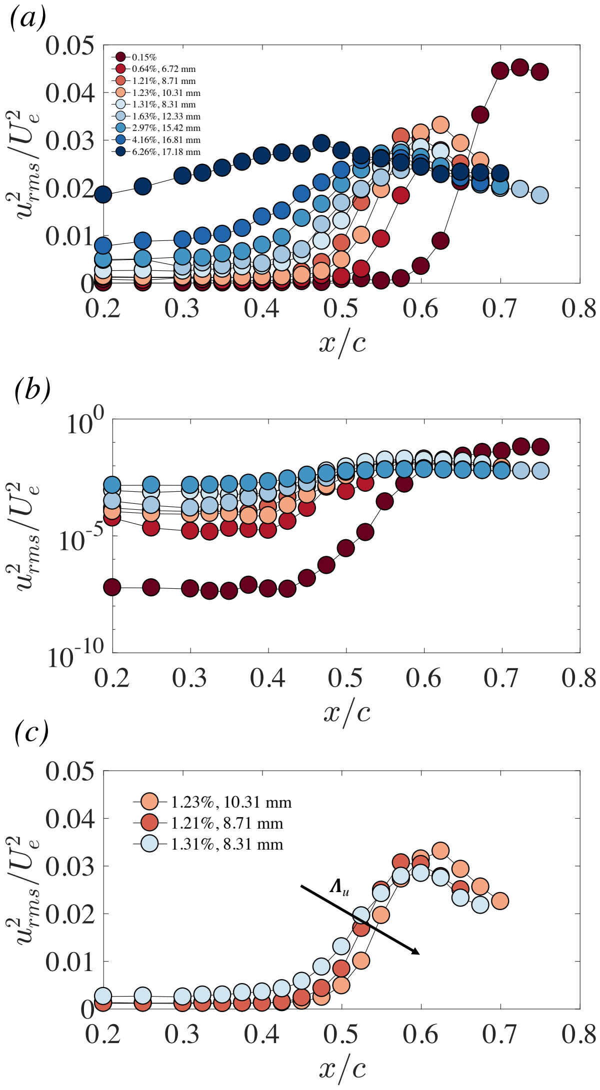

Figure 3. The disturbance energy growth for a) integrated over the entire energy spectrum and b) integrated over the frequency range of the most amplified wave packet and c) configurations with are latively fixed Tu and varying Λ_u.

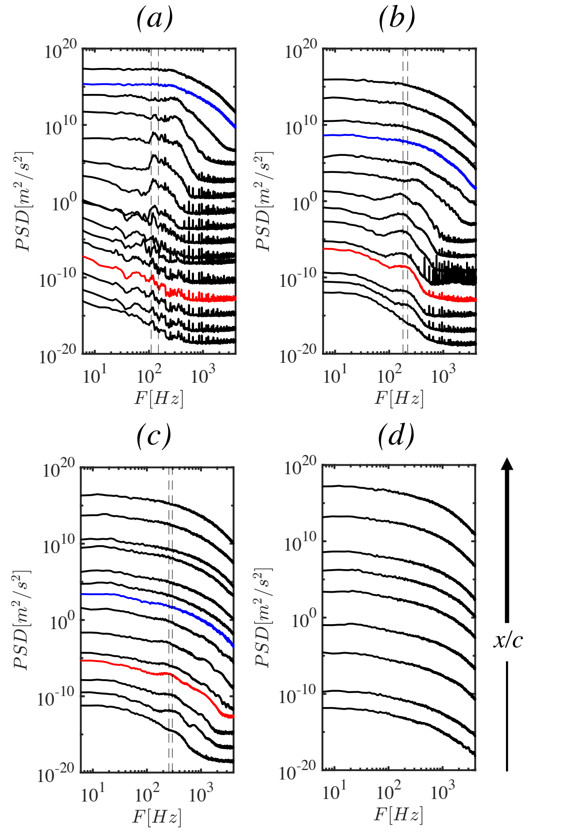

Figure 4. Chordwise evolution of the PSD. Frequency bands correspond to the vertical dashed lines which indicate the most amplified frequency band used in the stability analysis in the following section. Red and blue curves denote x_S and x_R, respectively. NB: Spectra are separated by an order of magnitude for clarity. a) Tu = 0.15%. Frequency band: [110-150 Hz]; b) Tu = 1.21%. Frequency band: [180-220 Hz]; c) Tu = 2.97%. Frequency band: [255-295 Hz]; d) Tu = 6.28%;

higher initial level of disturbance energy in the boundary layer and has been also observed by Hosseinverdi (2014), however in their work, the saturation of the energy growth was found to be independent of Λ_u. Based on the experimental observations here and past numerical simulations, an effect of integral length scale could be present and further investigation is warranted. However, it is likely that the effect will be small compared to the Tu, in light of the results here and Hosseinverdi & Fasel (2019).

Results of the linear stability analysis are presented Fig. 5, where an overlaid plot between PSD from experiment and α_i shows that LST is capable of predicting the most amplified frequencies from experiment, even in the presence of elevated levels of Tu (NB. Only two configurations are presented for brevity). Furthermore, the eigenfunctions of the most amplified frequency predicted by LST are presented in Fig. 6a,b, and are in acceptable agreement with the experiment for the filtered (for the most amplified frequency band) fluctuating streamwise velocity profile in the wall-normal direction. The eigenfuction exhibits two distinct peaks at approximately y/δ_1 = 1, corresponding roughly to the inflection point and y/δ_1 = 0.3, which is indicative of a viscous modal instability (Veerasamy *et al.*, 2021). Rist & Maucher (2002) showed that LSBs with smaller wall normal-distances could exhibit a viscous modal instability. Therefore, even when the LSB is subjected to elevated levels of freestream turbulence, LST can predict the most amplified frequencies and eigenfunctions. This suggests that a modal instability is still present at elevated levels of freestream turbulence when the bubble is present. Furthermore, the unfiltered (Fig 6d) distrubance profiles agree remarkably well with the theoretical optimal perturbation profile (Luchini, 2000) for configurations with Tu > 1%. Although not presented in the present paper, all configurations where Tu > 1% exhibit agreement with the optimal perturbation profile at multiple chordwise positions, demonstrating self similarity of the disturbance profiles over most of the boundary layer. With the only exception being outside of the boundary layer, with u_{rms}/u_{max} not tending to zero since freestream turbulence is present, in contrast to theory, which has no freestream disturbances outside of the boundary layer. In configurations where Tu < 1% (Fig 6c), experimental disturbance profiles do not agree with theory, implying that only a modal instability was present. Furthermore, all configurations subjected to freestream disturbance levels of Tu < 3% show agreement with LST. Therefore, the results imply the coexistence of both modal and non-modal instability mechanisms, confirming the observations made by Hosseinverdi & Fasel (2019). The damping of the disturbance growth

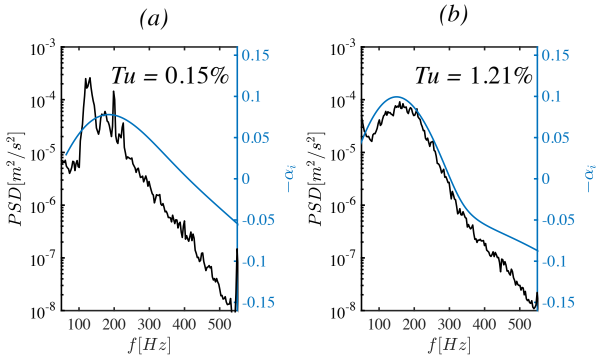

Figure 5. Comparison between the amplified frequencies predicted by LST to the experimental spectra for (a) Natural case ($x = 0.400c$); (b) $Tu = 1.21\% \Lambda_u = 8.7mm$ ($x = 0.425c$); NB: Two different $y-$axes for α_i and the power from the PSD, therefore direct comparisons between the two are not be made.

of the modal instabilities (cf. Fig. 3b) is attributed to the streaks modifying the mean flow.

Further insights can be obtained upon examination of the contours of the non-dimensional frequency (Ω) and α_i as a function of the Reynolds number plotted in Fig. 7 for the baseline configuration and a forced one. For lower Tu, a larger range of unstable frequencies is present, which is due to the inflectional point being further away from the wall. Upon inspection of the contours of the LST growth rates (Fig. 7a), a dependence on Re_{δ_1} is observed, suggesting that viscosity needs to be considered in the LST calculation in the fore position of the LSB. Moreover, increasing Tu results in the range of unstable frequencies to decrease and the Reynolds number dependence to increase (Fig. 7b), due the inflection point shifting closer towards the wall, resulting in an increased effect of viscosity. For example, the increased dependence of α_i on Re_{δ_1} with increased Tu, is clearly demonstrated in Figs. 7c and d where the unexcited bubble converges at $Re_{\delta_1} \approx 8000$ compared to $Re_{\delta_1} \approx 13000$ for the elevated levels of Tu. This result implies that invicid LST calculations are unsuitable to accurately model the stability in the fore position of the LSB (especially in the presence of elevated levels of FST) at the low values of Re_{δ_1} considered in the present work.

CONCLUSION

The present investigation examined the effects of varying the freestream turbulence intensity and integral length scale on the flow development and transition in a laminar separation bubble. The current work provides experimental evidence on the coexistence of modal and non-modal instabilities in a laminar separation bubble. It is shown, through experiment and theory, that even at relatively high/moderate turbulence intensity levels the modal instability is still operational in an LSB and the primary growth can be satisfactorily predicted with the Orr-Sommerfeld formulation. The damping of the streamwise growth of disturbances is due to the presence of streaks caused by the elevated levels of freestream turbulence, which modify the mean flow topology of the bubble through the introduction of non-modal disturbances (streaks) into the boundary layer. A dependence of α_i on Re_{δ_1} is observed, suggesting that viscosity effects need to be considered in LST calculations in the fore position of the LSB.

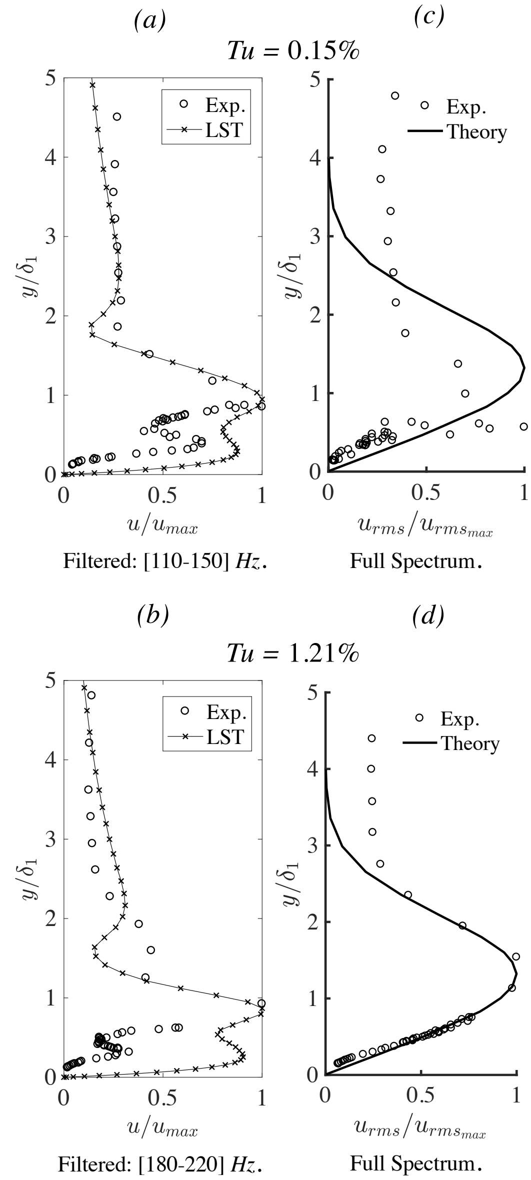

Figure 6. Experimental filtered disturbance profiles in the wall-normal direction compared to the eigenfunction for the most amplified frequency from LST. Experimental streamwise disturbance profiles are computed by applying a bandpass filter corresponding to the lost amplified frequency band from the PSD (a,c). Unfiltered experimental disturbance profiles compared to optimal perturbation theory (b, d).

REFERENCES

Boutilier, Michael SH & Yarusevych, Serhiy 2012 Separated shear layer transition over an airfoil at a low Reynolds number. *Physics of Fluids* **24** (8), 084105.

Breuer, Michael 2018 Effect of inflow turbulence on an airfoil flow with laminar separation bubble: An LES study. *Flow, Turbulence and Combustion* **101** (2), 433–456.

Fransson, Jens HM, Matsubara, Masaharu & Alfredsson, P Henrik 2005 Transition induced by free-stream turbulence. *Journal of Fluid Mechanics* **527**, 1–25.

Fransson, Jens HM & Shahinfar, Shahab 2020 On the effect of free-stream turbulence on boundary-layer transition. *Journal of Fluid Mechanics* **899**.

Häggmark, CP, Bakchinov, Andrey A & Alfredsson, P Henrik 2000 Experiments on a two–dimensional laminar separation

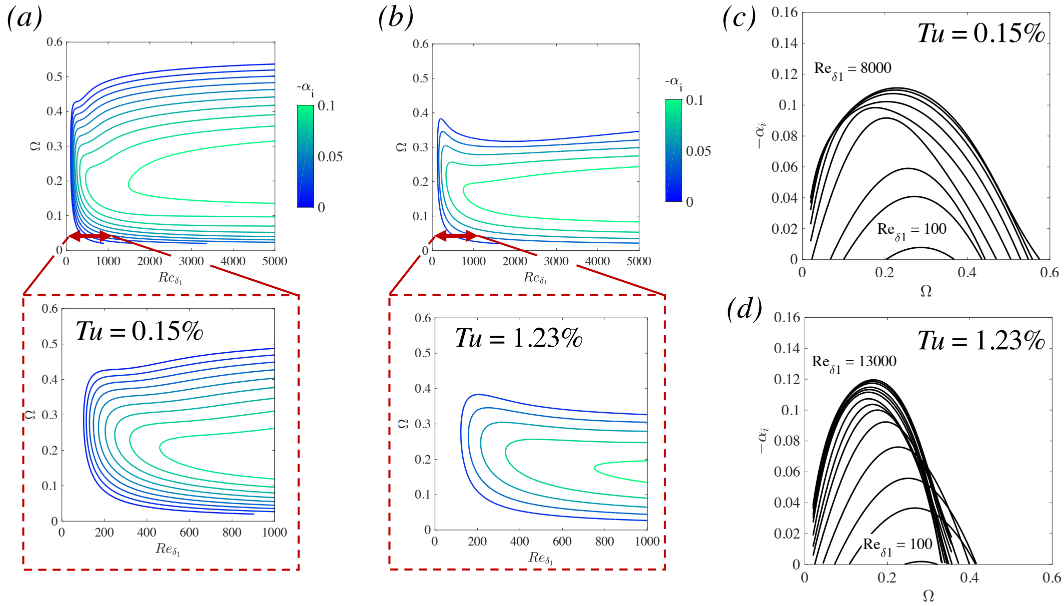

Figure 7. Contours of LST predicted spatial growth rates (α_i) as a function of the dimensionless frequency Ω and Reynolds number (Re_{δ_1}) for the natural case for a mean velocity profile at $x = 0.400c$ (a) and an elevated freestream turbulence case for a mean velocity profile at $x = 0.425c$ (b). The dependence of α_i on Re_{δ_1} is presented in (c) and (d) for the natural and exited case, respectively. In both configurations the initial value of $Re_{\delta_1} = 100$ and continues up until the maximum α_i converges within 2%.

bubble. *Philosophical Transactions of the Royal Society of London. Series A: Mathematical, Physical and Engineering Sciences* **358** (1777), 3193–3205.

Hosseinverdi, Shirzad 2014 Influence of free-stream turbulence on laminar-turbulent transition in long laminar separation bubbles: Direct Numerical Simulations. Master's thesis.

Hosseinverdi, Shirzad & Fasel, Hermann 2019 Numerical investigation of laminar–turbulent transition in laminar separation bubbles: the effect of free-stream turbulence. *Journal of Fluid Mechanics* **858**, 714–759.

Istvan, Mark S & Yarusevych, Serhiy 2018 Effects of free-stream turbulence intensity on transition in a laminar separation bubble formed over an airfoil. *Experiments in Fluids* **59** (3), 52.

Jaroslawski, Thomas, Forte, Maxime, Moschetta, Jean-Marc, Delattre, Gregory & Gowree, Erwin R 2022 Characterisation of boundary layer transition over a low Reynolds number rotor. *Experimental Thermal and Fluid Science* **130**, 110485.

Kurelek, John William, Kotsonis, Marios & Yarusevych, Serhiy 2018 Transition in a separation bubble under tonal and broadband acoustic excitation. *Journal of Fluid Mechanics* **853**, 1–36.

Luchini, Paolo 2000 Reynolds-number-independent instability of the boundary layer over a flat surface: optimal perturbations. *Journal of Fluid Mechanics* **404**, 289–309.

Marxen, Olaf & Henningson, Dan S 2011 The effect of small-amplitude convective disturbances on the size and bursting of a laminar separation bubble. *Journal of Fluid Mechanics* **671**, 1–33.

Matsubara, M & Alfredsson, P Henrik 2001 Disturbance growth in boundary layers subjected to free-stream turbulence. *Journal of Fluid Mechanics* **430**, 149.

Rist, Ulrich & Maucher, Ulrich 2002 Investigations of time-growing instabilities in laminar separation bubbles. *European Journal of Mechanics-B/Fluids* **21** (5), 495–509.

Simoni, Daniele, Lengani, Davide, Ubaldi, Marina, Zunino, Pietro & Dellacasagrande, Matteo 2017 Inspection of the dynamic properties of laminar separation bubbles: free-stream turbulence intensity effects for different Reynolds numbers. *Experiments in Fluids* **58** (6), 66.

Veerasamy, Dhamotharan, Atkin, Chris J & Ponnusami, Sathiskumar A 2021 Aerofoil wake-induced transition characteristics on a flat-plate boundary layer. *Journal of Fluid Mechanics* **920**.

Volino, Ralph J 1997 A new model for free-stream turbulence effects on boundary layers. In *Turbo Expo: Power for Land, Sea, and Air*, , vol. 78705, p. V003T09A015. American Society of Mechanical Engineers.

Yarusevych, Serhiy & Kotsonis, Marios 2017 Steady and transient response of a laminar separation bubble to controlled disturbances. *Journal of Fluid Mechanics* **813**, 955–990.